Numerical approximation of linear operator equations using a generalized Fourier series: ordinary and partial differential equations with boundary conditions

Theodore V. Hromadka II

Williamson and Schmid, Irvine, CA, and Department of Mathematics, California State University, Fullerton, CA, USA

Robert J. Whitley

Department of Mathematics, University of California, Irvine, CA, USA

Many important engineering problems fall into the category of being linear operators with supporting conditions. In this paper an inner product and norm are used to numerically approximate the linear operator equation by use of generalized Fourier series. The resulting approximation is the "best" approximation in that a least squares error is minimized simultaneously for both fitting the problem's boundary conditions and satisfying the linear operator relationship (the governing equations) over the problem's domain. Because the numerical approximation technique involves a well-defined inner product, the approximation error can be evaluated by using Bessel's inequality. Minimization of the approximation error is subsequently achieved with respect to a weighting of the inner product components and the addition of basis functions used in the approximation. In this paper the numerical modelling technique is applied toward evaluating linear operation relationships such as ordinary and partial differential equations with fixed boundary equations. Nonlinear operators are also considered that can be approximated as being stepwise linear for portions of the problem domain (space or time). Additionally, different types of basis functions are considered, namely, the usual finite element trial function class, and also basis functions that span the domain with nonzero values (almost everywhere) such as polynomials, among others. Application of the generalized Fourier series approach to solving the problem of coupled heat and soil water flow in freezing soils demonstrates the utility of this numerical modelling technique.

Keywords: linear operator, generalized Fourier series, ordinary and partial differential equations

Introduction

The development of the considered numerical approximation technique is presented in detail in Ref. 1. Although a brief summary of the mathematical underpinnings of the technique is provided below, the reader is referred to Ref. 1 for in-depth considerations.

An inner product for the solution of linear operator equations

The setting for solving a linear operator equation with boundary conditions by means of an inner product is as follows:[1] Let Ω be a domain in R^m with boundary Γ and denote the closure of Ω by cl (Ω). Consider the Hilbert space $L^2(\text{cl}\,(\Omega), d\mu)$, which has inner product $(f, g) = \int fg\, d\mu$. A method to define the inner product for the development of a generalized Fourier series is to let μ be measure μ_1 on Ω and another measure μ_2 on Γ. For example, one choice for a plane region would be for μ_1 to be the usual two-dimensional Lebesgue measure $d\Omega$ on Ω and for μ_2 to be the usual arc length measure $d\Gamma$ on Γ. Then an inner product is given by

$$(f, g) = \int_{\Omega} fg\, d\Omega + \int_{\Gamma} fg\, d\Gamma \qquad (1)$$

Consider a boundary value problem consisting of a linear operator L defined on domain $D(L)$ contained in

Address reprint requests to Dr. Hromadka, Director of Water Resource Engineering, Williamson and Schmid, 17782 Sky Park Boulevard, Irvine, CA 92714, USA.

Received 7 February 1989; accepted 3 July 1989

Because the $\langle g_j \rangle^m$ are orthonormalized and the inner product (u, v) is well-defined, the coefficients λ_j of (8) are immediately determined by the generalized Fourier constants, λ_j^*, where

$$\lambda_j^* = (g_j, \phi) \qquad j = 1, 2, \ldots, m \tag{11}$$

Thus

$$\phi_m^* = \sum_{j=1}^{m} \lambda_j^* g_j = \sum_{j=1}^{m} (g_j, \phi) g_j \tag{12}$$

is the "best" approximation of ϕ, in the space S^m, for the considered inner product.

Approximation error evaluation

From the generalized Fourier series approach and the definition of the inner product, Bessel's inequality applies. That is, for any dimension m,

$$(\phi, \phi) \geq \sum_{j=1}^{m} (g_j, \phi)^2 = \sum_{j=1}^{m} \lambda_j^{*2} \tag{13}$$

where

$$(\phi, \phi) = \int_\Gamma (\phi_b)^2 \, d\Gamma + \int_\Omega (L\phi)^2 \, d\Omega$$

$$= \int_\Gamma (\phi_b)^2 \, d\Gamma + \int_\Omega h^2 \, d\Omega \tag{14}$$

Equation (14) forms an upper bound to the sum of $(g_j, \phi)^2$ as the dimension m increases. Consequently, one may interact with the approximation effort by carefully adding functions to the $\langle g_j \rangle^m$ in order to best reduce the error computed by Bessel's inequality.

The weighted inner product

In the inner product of (4), equal weight is given to the various requirements imposed on the best approximation function ϕ_m from the space S^m spanned by the m linearly independent basis functions $\langle f_j \rangle^m$. Namely, the L^2 error in satisfying the linear operator relationship over Ω is weighted equally as the L^2 error in satisfying the problem's boundary conditions.

Due to the limitations of computer power, only a finite number of basis functions can be used for approximation purposes, and so an argument is made to weight the terms that compose the inner product differently. For $0 < \epsilon < 1$, one weighting of (4) is simply[1]

$$(u, v, \epsilon) = \epsilon \int_\Gamma uv \, d\Gamma + (1 - \epsilon) \int_\Omega Lu \, Lv \, d\Omega \qquad 0 < \epsilon < 1 \tag{15}$$

In (15) an ϵ-value close to 1 would weight the approximation function ϕ_m of S^m toward satisfying the problem's boundary conditions rather than satisfying the linear operator. Similarly, an ϵ-value close to 0 would weight the ϕ_m approximation toward satisfying the linear operator relationship over Ω.

It is noted that (15) is still an inner product for a given choice of ϵ and will be used to develop the generalized Fourier series using (6). And as the dimension S^m increases, the Bessel's inequality still applies in that $\chi = \chi_\epsilon$ and

$$\chi_\epsilon = 0 \qquad \textit{implies} \qquad \|\phi_m - \phi\|_\epsilon = (u, v, \epsilon)^{1/2} = 0 \tag{16}$$

The choice of basis functions

The inner product of (15) demonstrates, as one would expect, that the "best" approximation ϕ_m in S^m to ϕ can be only as "good" as the space S^m permits. Hence the choice of the underlying basis functions, $\langle f_j \rangle^m$, dictates the goodness of the approximation to be anticipated. For example, by choosing the $\langle f_j \rangle^m$ such that each element f_j satisfies the operator, then the domain integral of (15) vanishes, and a boundary integral equation method results (for example, Hromadka and Yen[4] use analytic functions and the inner product of (15) to numerically approximate ideal fluid flow problems in two-dimensional domains).

In this paper, two types of basis functions are considered: basis functions that are nonzero almost everywhere on Ω (such as polynomials) and basis functions such as the type usually employed in finite element methods (that is, they are nonzero only in a prescribed finite element).

Numerical approximation of integrals and approximation in R^n

In numerical approximation of the integrals in (15) the boundary Γ and domain Ω integrals are usually estimated in evaluating the integrand at each point of a dense partitioning and weighting the integrand point value according to the Riemann integral area (or length) associated with the evaluation point. In this fashion, as the density of evaluation points increases (and as the evaluation point–associated area or length decreases), the numerical approximation error of the integrals decreases. Assuming that the numerical integration approximation utilizes a partition of the domain Ω (or boundary Γ) into equal evaluation point–associated areas (or boundary lengths), the numerical integration effort is equivalent to resolving the generalized Fourier series problem as a vector space problem in R^n, where n is the total number of evaluation points used over $\Omega \cup \Gamma$, and the inner product of (15) is the well-known dot product between n-dimensional vectors in R^n.

The above equivalence between the numerical approximation of the inner product integrals and solving a vector space problem in R^n also indicates that increasing computational effort in a region of the problem (by using a more detailed discretization with finite elements) is equivalent to a spatial weighting of the inner product integrals, where more weight is added according to the density of the evaluation points.

1. the approximation of the solution space by the space S^m spanned by the selected m basis functions, $\langle f_j \rangle^m$;
2. the use of the L^2 norm in minimizing approximation error; and
3. the approximation of the space S^m by the space R^n (that is, the representation of the basis functions, $\langle f_j \rangle^m$, by the vectors in R^n, $\langle F_j \rangle^m$).

Example 1

The above numerical technique is applied to the one-dimensional ordinary differential equation $y'' + y = 0$ with boundary conditions $y(0) = 0$ and $y(\pi/2) = 1$. The inner product of (15) is used with $\epsilon = 0.50$ and with the basis functions selected from $\langle 1, x, \sqrt{x}, \sin x, \cos x, x \sin x, x \cos x, e^x, x^2, x^3, x^4, x^5 \rangle$. That is, finite element–type basis functions are not currently being considered. For prescribed subsets of basis functions the approximation results are shown in *Figure 2*. The utility of ϵ weighting factor in the inner product is shown in *Figure 3*, where several ϵ values are used, demonstrating the weighting of either the operator or the boundary conditions. The corresponding success of solving the governing operator is shown in *Figure 4* for various ϵ values. It is seen in *Figure 4* that as the inner product weighting is focused toward solving the operator $L(\phi) = 0$, the approximation effort is indeed weighted towards zero error in the operator space.

Example 2: finite elements

We now consider finite element–type basis functions, which are polynomials in a finite element and zero elsewhere. That is,

$$\hat{\phi}(x) = \sum_{j=1}^{m} N_j(x)\, \hat{\phi}_j$$

where $N_j(x)$ is a basis function that equals 1 at nodal point j and zero at all other nodes; m is the total number

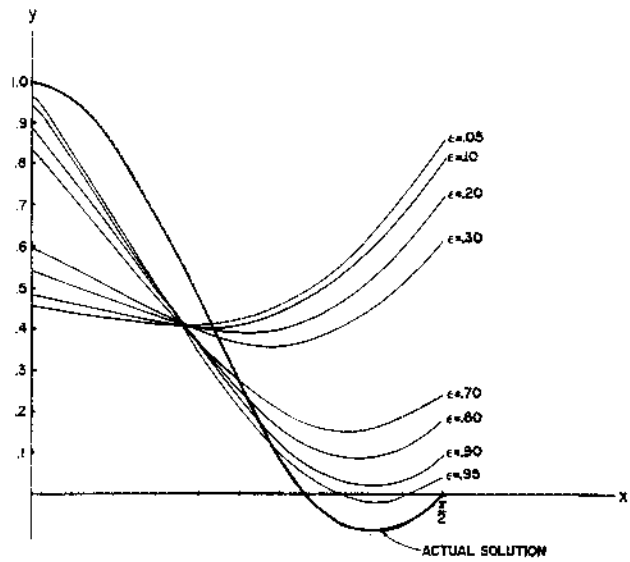

Figure 3. Approximation results in Figure 2 for various ϵ ($x \sin x$ deleted from basis functions)

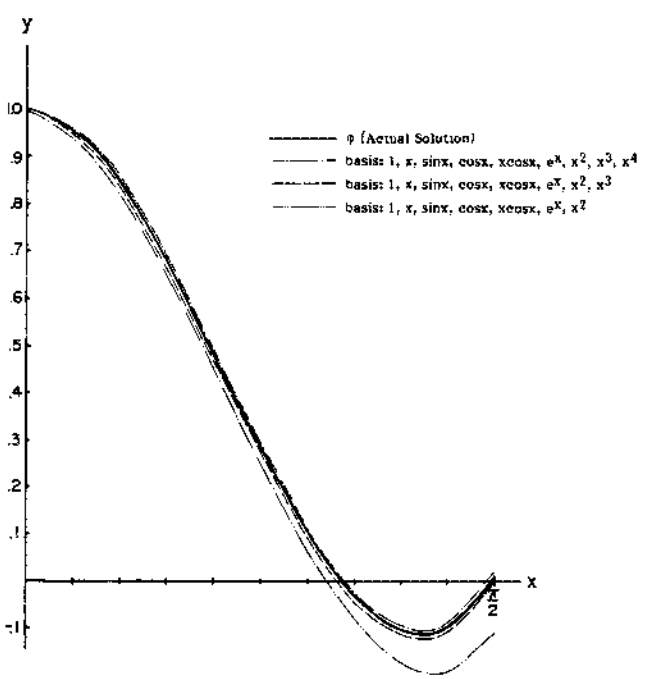

Figure 2. Approximation results for various bases, of $y'' + y = 0$

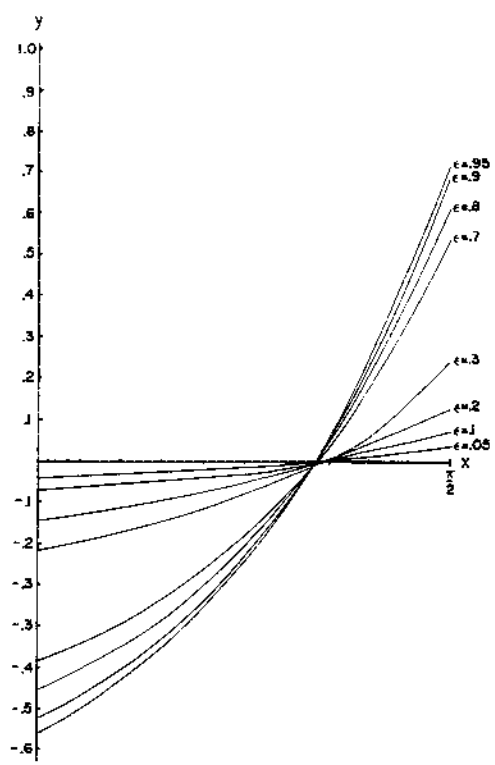

Figure 4. Approximation results in satisfying the operator $y'' + y = 0$ for various basis functions

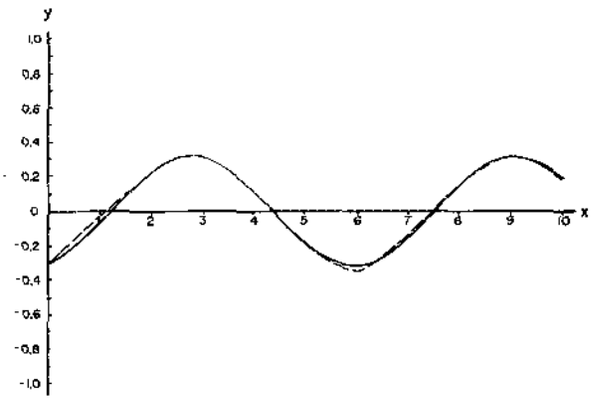

Figure 9. Solving $y'' + 3y' + y = \sin x$ by using quadratic trial functions with nodes at 0, 1, 2, . . . , 10. The solid curve is the exact solution; the dashed curve is the approximation

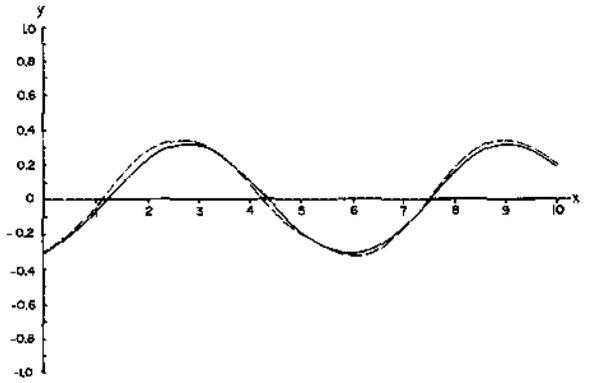

Figure 10. Solving $y'' + 3y' + y = \sin x$ by using quadratic trial functions with nodes at 0, 0.1, 0.2, . . . , 1, 2, 3, . . . , 10. The solid curve is the exact solution; the dashed curve is the approximation

For this type of problem the linear operator equation is

$$L\phi = \frac{\partial^2 \phi}{\partial x^2} + \frac{\partial^2 \phi}{\partial y^2} = 0 \qquad \text{in } \Omega \tag{23}$$

with boundary conditions $\phi = \phi_b$ on boundary Γ.

By using the concepts summarized previously, the domain Ω is discretized into triangular finite elements, Ω^e, such as those shown in *Figure 1*. For our problem the triangular element is based on the usual quadratic basis function, which utilizes six nodal points. The quadratic basis functions, $N_i^e(x, y)$, are defined for each node i such that in finite element e (which contains node i),

$$N_i^e(x, y) = \begin{cases} a_{i0}^e + a_{i1}^e x + a_{i2}^e y + a_{i3}^e xy + a_{i4}^e x^2 + a_{i5}^e y^2 & (x, y) \in \Omega^e \\ 0 & (x, y) \notin \Omega^e \end{cases} \tag{24}$$

where $N_i(x, y) = 1$ at nodal point i and $N_i^e(x, y) = 0$ at all other nodal points. Additionally, $N_i^e(x, y)$ assumes nonzero values only in finite elements that contain node i.

Because the selected finite element basis functions are quadratic polynomials in Ω^e,

$$LN_i^e(x, y) = \begin{cases} 2a_{i4}^e + 2a_{i5}^e & (x, y) \in \Omega^e \\ 0 & (x, y) \notin \Omega^e \end{cases} \tag{25}$$

and therefore for nodes i and j in Ω^e,

$$\int_\Omega LN_i^e(x, y)\, LN_j^e(x, y)\, d\Omega = (2a_{i4}^e + 2a_{i5}^e)(2a_{j4}^e + 2a_{j5}^e) \int_{\Omega^e} d\Omega \tag{26}$$

From (25) and (26) it is seen that the use of interior evaluation points is greatly simplified owing to the exact integration of the selected basis functions.

The particular precision of the integration of basis function contributions in (26) is due to the selection of the basis functions. Other choices of basis functions might not result in such precision. If the above finite element basis functions are mixed with basis functions such as polynomials defined over the entire domain or functions such as logarithms or rational functions, among others, then the use of interior evaluation points is once again necessary in order to properly approximate the integrals.

Application: generalized Fourier series model of two-dimensional coupled heat and soil water transport in algid soils

In this section we develop a two-dimensional model of coupled heat and soil water flow in algid soils. Numerical solution is by the use of generalized Fourier series with basis functions of finite element type and rational functions. Solution of the phase change process is approximated by an isothermal approach, and phenomenological equations are assumed for processes occurring in freezing or thawing zones. The numerical model is verified against experimental one-dimensional freezing soil column data and experimental two-dimensional soil thawing tank data as well as two-dimensional soil water flow data.

Numerical modelling of coupled heat and moisture transport in freezing and thawing soils has been the subject of a number of investigations. Modelling efforts reported in the literature primarily deal with numerical approximations of heat and soil water transport and involve finite difference or finite element numerical analogs to solve the governing equations. These numerical models are reviewed by Guymon et al.,[6] (1980), Hopke,[7] and O'Neill,[8] among others.

The purpose of this section is to present an application of generalized Fourier series to model dynamic two-dimensional coupled heat and soil water transport in freezing and thawing soils. The model is based upon the theoretical concepts employed in Ref. 9, but the

Figures 17a and *17b*, whereas a two-dimensional problem interpolation is shown in *Figure 17c*.)

The algorithms for the several transport processes are shown in *Figures 18–20*. *Figure 18* shows the heat flow model, and *Figure 19* illustrates the soil water flow model. After time step Δt, phase change effects are then estimated according to *Figure 20*. Further details regarding the soil water freezing algorithms and budgets can be found in Ref. 23.

Model verifications

Linearized decoupled problems may be solved analytically to determine the accuracy of the soil water and heat flow generalized Fourier series models. Analytical solutions of freezing soil or bulk water are for one-dimensional columns. Thus the accuracy of a two-dimensional model may be studied by solving one-dimensional column problems. Several column tests were made for both unsaturated soil moisture transport and heat transport, with and without phase change. For heat transport alone, errors in the position of isotherms and particularly the freezing isotherm were less than 5% for relatively fine spatial discretization and fairly large time steps. Relative errors could be reduced to less than 2% for smaller time steps. Unsaturated soil moisture transport in a vertical column was evaluated by comparison to a quasi-analytical solution as discussed in Ref. 9. Close agreement was obtained between models.

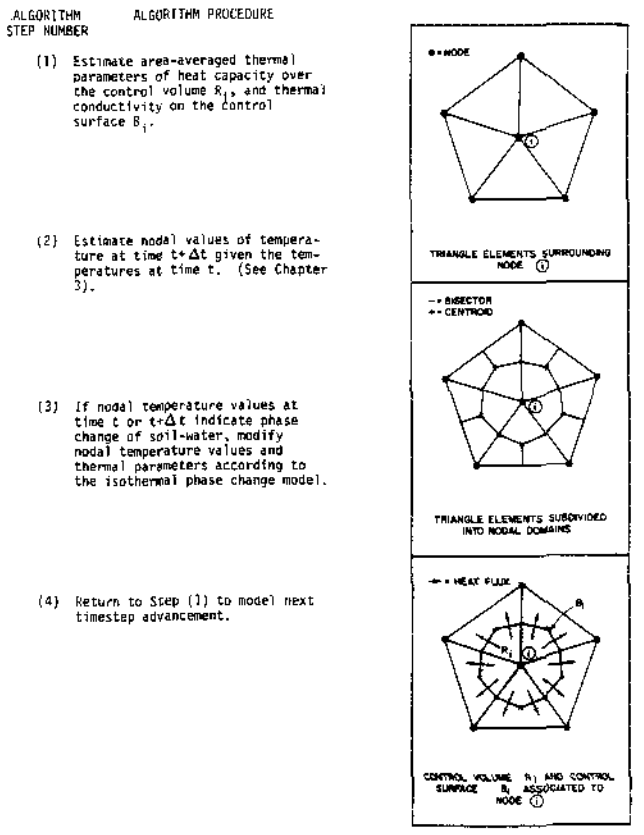

Figure 18. Heat flow model

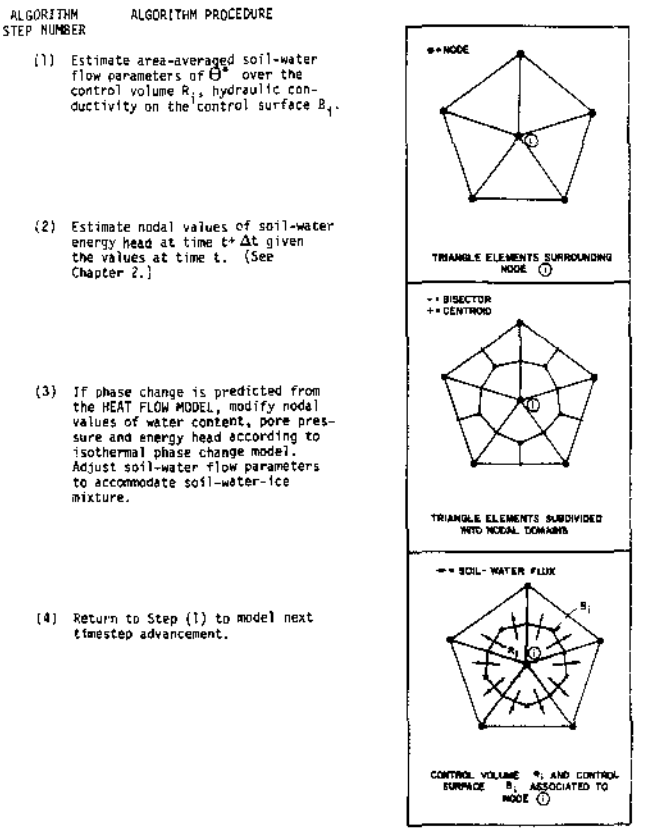

Figure 19. Soil water flow model

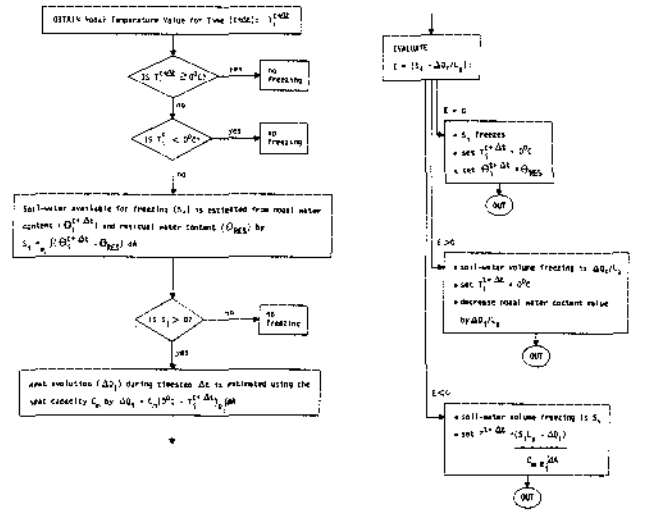

Figure 20. Isothermal soil-water freezing model

The two-dimensional model was compared to one-dimensional model solutions and one-dimensional laboratory soil column tests. The one-dimensional model has been extensively verified against soil column data and field data.[19,21,24] *Figure 21* shows an example comparison for a coupled heat and soil water transport problem involving Fairbanks silt. In this example the column top was subjected to a -5°C temperature (at

eralized Fourier series approach provided significant improvement in computational accuracy over the more traditional Galerkin finite element modelling approach as used in the cited publications.

Two-dimensional verification of the heat transport model includes comparison with field data for a laboratory sand tank.[27] The sand tank model consisted of a 3.92-m-wide by 1.28-m-deep tank of sandy silt that is over 4-m long to simulate two-dimensional thawing around a buried small-diameter hot pipe. The embankment is initially frozen. Sides and bottoms are insulated to provide zero heat loss (i.e., zero heat flux). The upper boundary condition and pipe temperature boundary conditions are measured data. Because of symmetry, only half the tank was analyzed, where at the pipe centerline, zero heat flux in the x-direction was assumed. A comparison of modelled and measured soil temperatures after one day of initiating hot fluid flow in the buried pipe is shown in *Figure 24*. In this problem the generalized Fourier series approach provided quicker computational results than the Galerkin finite element model, but with similar computational accuracy.

Coupled problem example

A vertical homogeneous soil column is discretized into two-dimensional finite elements as shown in *Figure 25*. The water table ($\psi = 0$) forms the lower boundary condition, with an initial condition of a 45° pore pressure head profile (see *Figure 25*). The top of the column is then instantly flooded by a water depth of 2 cm of water. The soil water modeling results are shown in *Figure 26*. To demonstrate the effects of soil water freezing, the same column is initialized at a temperature of 0.1°C. The top of the column is set to a temperature of −5°C. The modelling results are summarized in *Figure 27*, in which soil water pore pressures, temperatures, and ice contents are shown graphically.

Conclusions

Generalized Fourier series provides a convenient tool for the approximation of linear operator equations. In this paper the use of generalized Fourier series for numerically approximating one- and two-dimensional linear partial differential equations is considered. Special considerations are studied regarding R^n vector space representation of the underlying basis function vector space and the use of a weighted inner product.

Also seen in this study is a parallel between "boundary element" and "finite element" methods. Both of these popular numerical techniques are seen to occur in the generalized Fourier series model development by the proper choice of basis functions. Also seen is

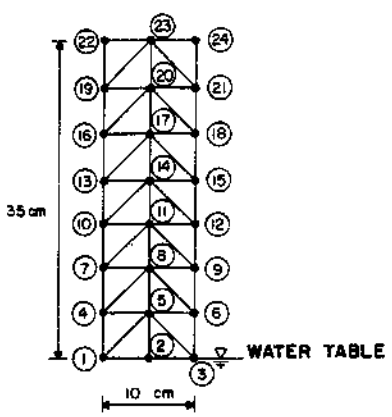

Figure 25. Soil water flow example problem

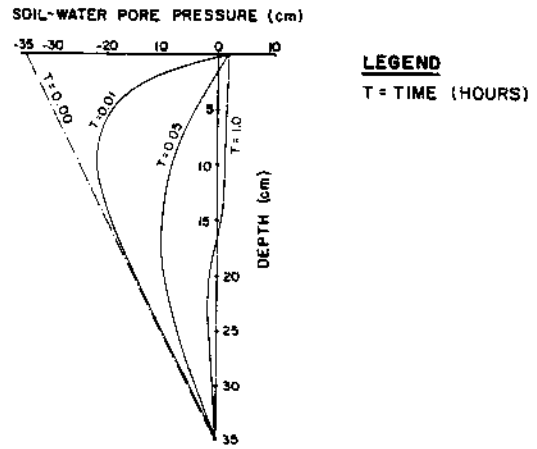

Figure 26. Solution of soil water flow example problem

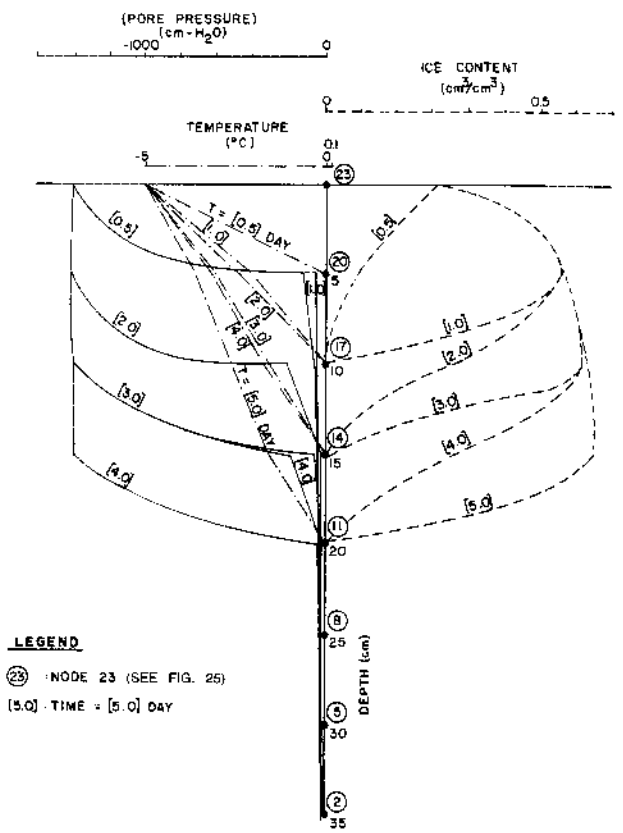

Figure 27. Solution of phase change problem